

Figure S1. Expression of key markers at each differentiation stage of GS iPSCs into HLCs.

(A) Gene expression of pluripotency (*OCT4* and *NANOG*) and definitive endoderm (DE) markers (*SOX17*, *GATA4* and *FOXA2*) in DE cells (n = 3). GS iPSCs were used as control, and the expression is normalized to that of *ACTB*. (B) Immunofluorescence staining of SOX17 and GATA4 in DE cells at the endpoint of stage I (n = 5); scale bar: 100 μ m. (C) RT qPCR analysis of hepatoblast markers (*AFP*, *HNF4A*, *CK18*, *CK19* and *TBX3*) at the stage II endpoint (n = 3). GS iPSCs were used as control, and the expression is normalized to that of *ACTB*. (D) Immunofluorescence staining of AFP and HNF4A in hepatoblasts at the endpoint of stage II (n = 5); scale bar: 50 μ m. (E) Representative immunoblots and quantification of OCT4, SOX17, AFP and ALB-like proteins in different stages of GS HLC differentiation. ACTB was used as the loading control (n = 3). (F) Representative dot blot of secreted ALB-like proteins in the culture supernatant during differentiation (n = 3). Data are expressed as mean \pm SEM; Student's *t*-test comparing to GS iPSCs (A, C and E); one-way ANOVA followed by Dunnett multiple-comparisons test versus GS iPSCs (F); *P* values are indicated.

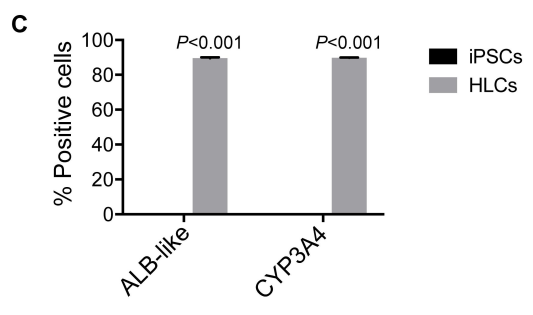
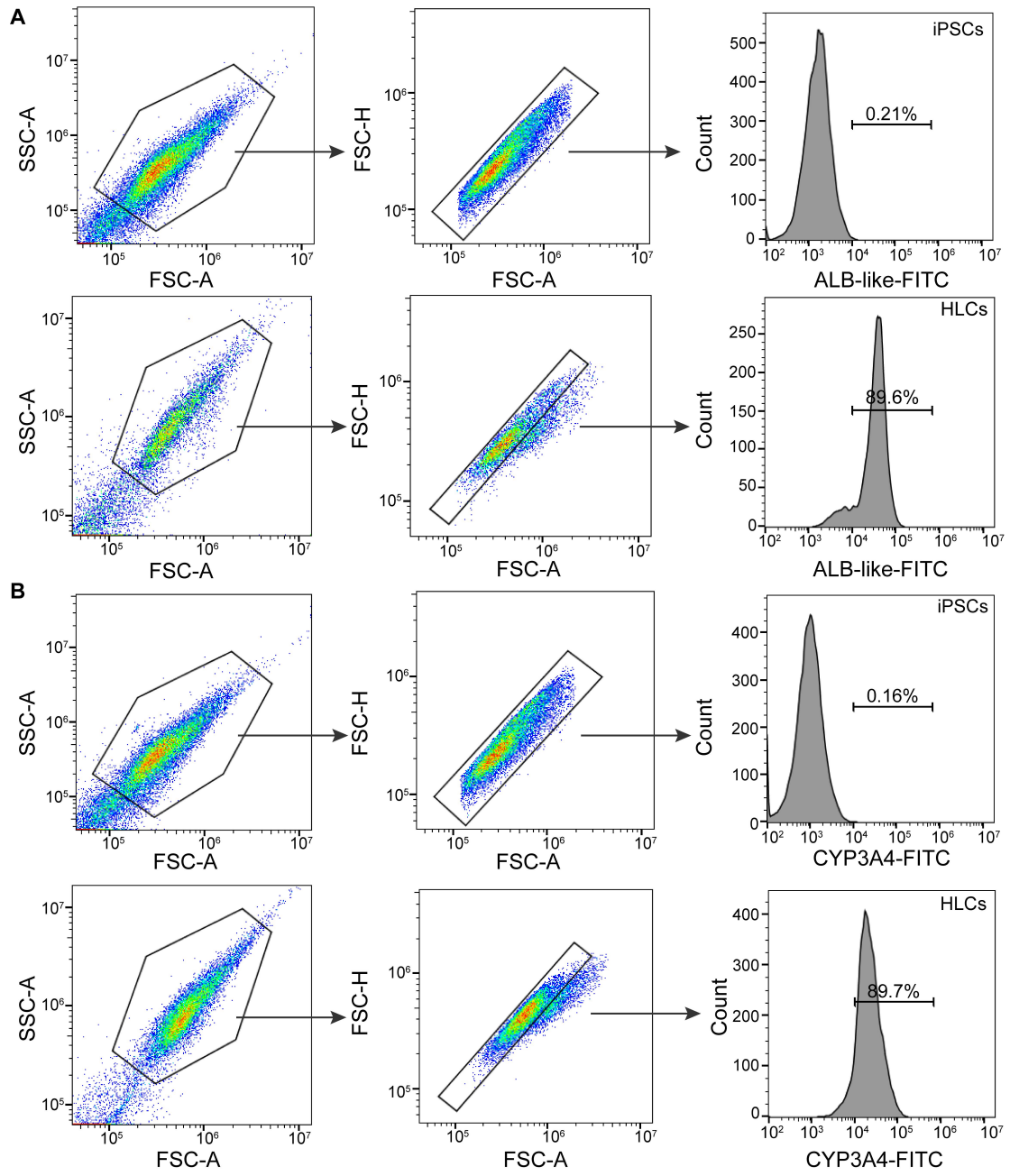


Figure S2. Gating strategy of flow cytometry in characterizing GS iPSCs and HLCs. Gating strategy of ALB-like (**A**) and CYP3A4 (**B**) in GS iPSCs and GS HLCs analyzed by flow cytometry. (**C**) Percentage of ALB-like- and CYP3A4-positive cells in GS iPSCs and HLCs (n = 3). Data are expressed as mean \pm SEM; Student's *t*-test between two comparisons; *P* values are indicated.

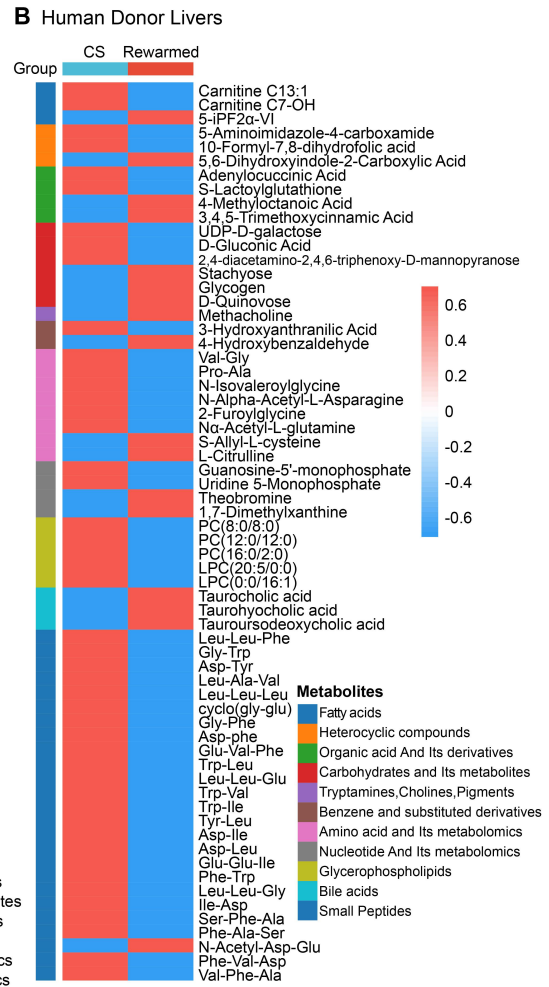
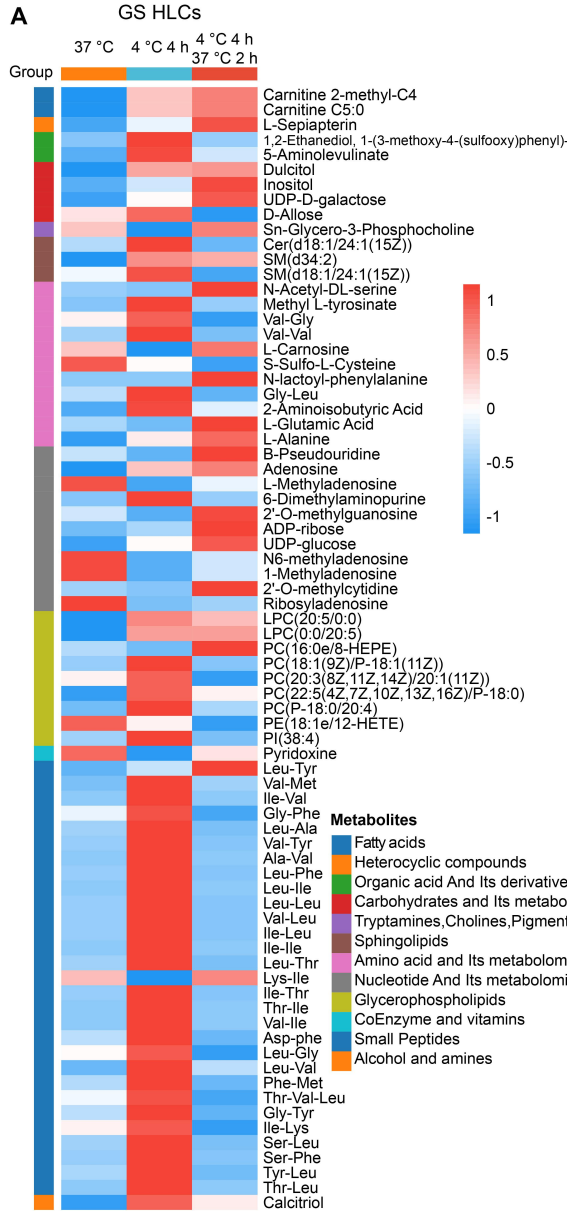


Figure S3. Metabolomic profiles of GS HLCs and human donor livers. (A) Heatmap showing differential metabolites of GS HLCs from the 37 °C, 4 °C 4 h and 4 °C 4 h-37 °C 2 h groups (n = 3 per group). (B) Heatmap showing differential metabolites of human donor livers during cold storage (CS) versus post-transplantation (Rewarmed; n = 10 per group).

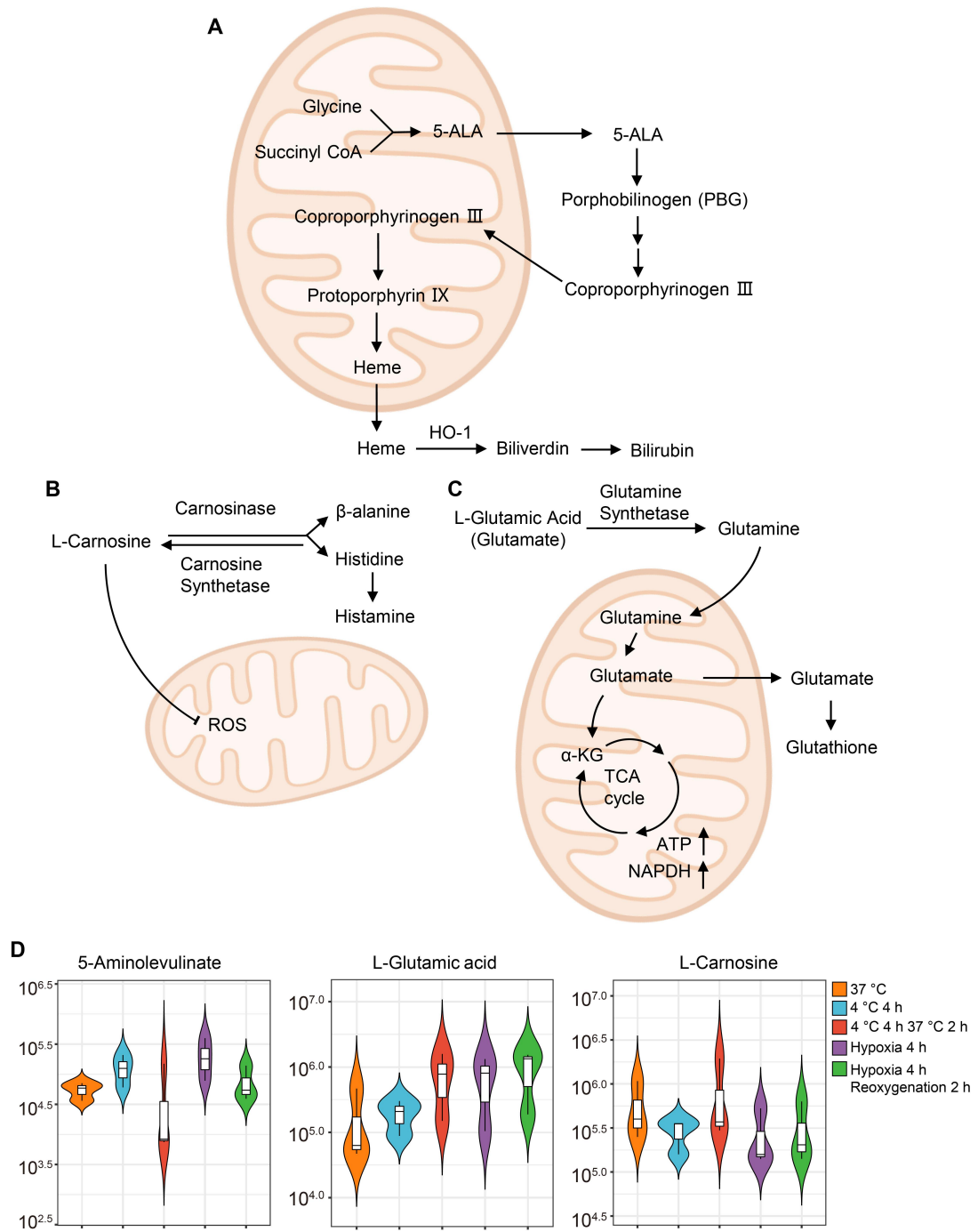


Figure S4. The Metabolic pathways and temperature/oxygen supply-induced changes of selected metabolites. (A-C) Schematic diagrams showing pathways of selected metabolites involved in mitochondrial metabolism (A, 5-aminolevulinate; B, L-Carnosine; C, L-Glutamic acid). (D) Violin Plots showing abundance of 5-aminolevulinate, L-carnosine and L-glutamic acid in GS HLCs at annotated conditions.

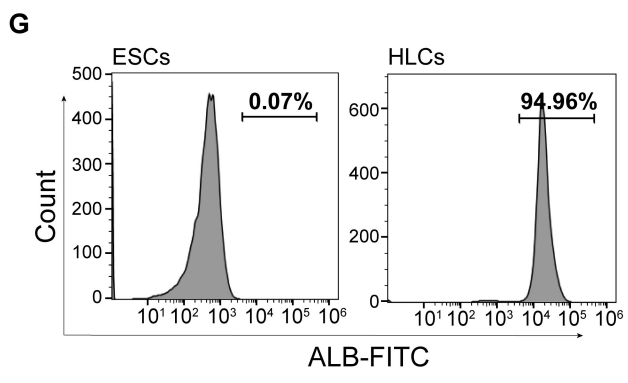
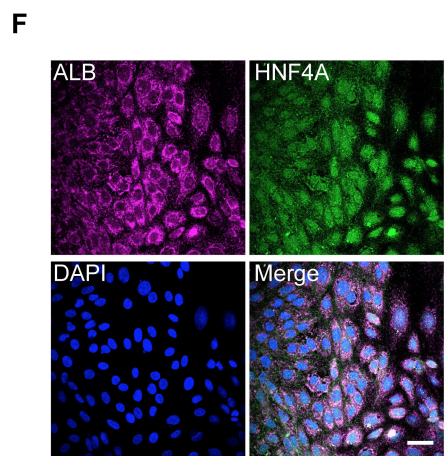
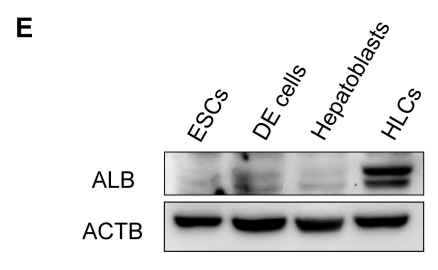
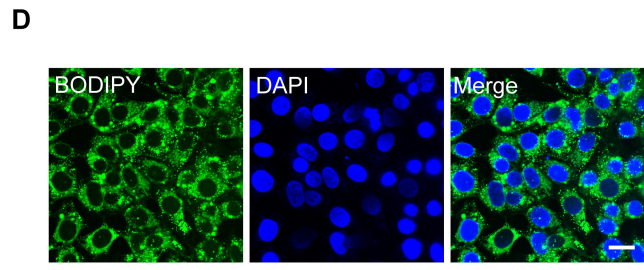
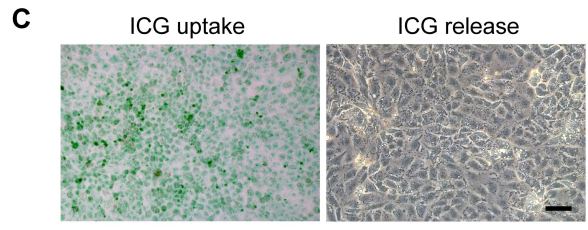
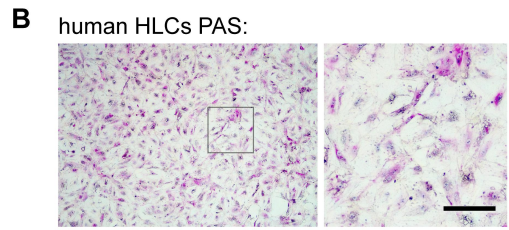
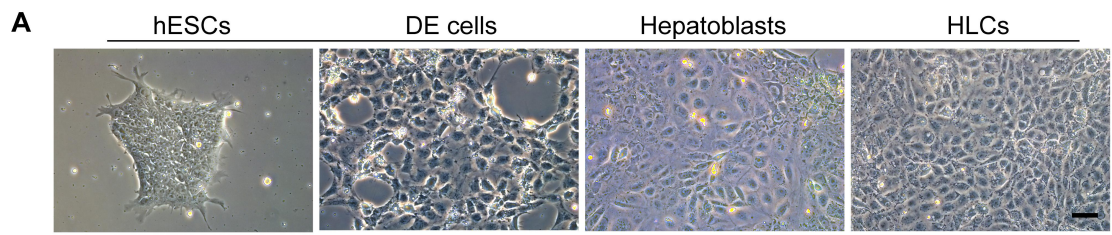


Figure S5. Differentiation of human embryonic stem cells (ESCs) into HLCs. (A)

Representative images showing sequential cellular morphological changes during human ESC differentiation into HLCs; scale bar: 100 μm . **(B)** PAS staining of glycogen storage in human HLCs (n = 5); scale bar: 50 μm . **(C)** Analysis of ICG uptake (left) and overnight release (right, n = 5); scale bar: 100 μm . **(D)** BODIPY staining of lipid droplets in human HLCs (n = 5); scale bar: 20 μm . **(E)** Representative immunoblots of human ALB and ACTB proteins in the endpoint of HLC differentiation (n = 3). **(F)** Immunofluorescence staining of HNF4a and ALB in human HLCs (n = 3); scale bar: 50 μm . **(G)** Percentage of ALB-positive cells in human ESC and HLC cultures analyzed by flow cytometry (n = 3).

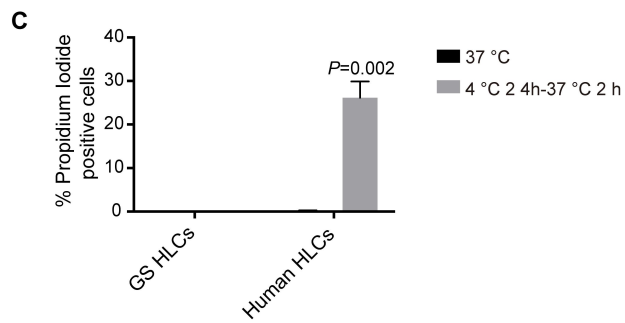
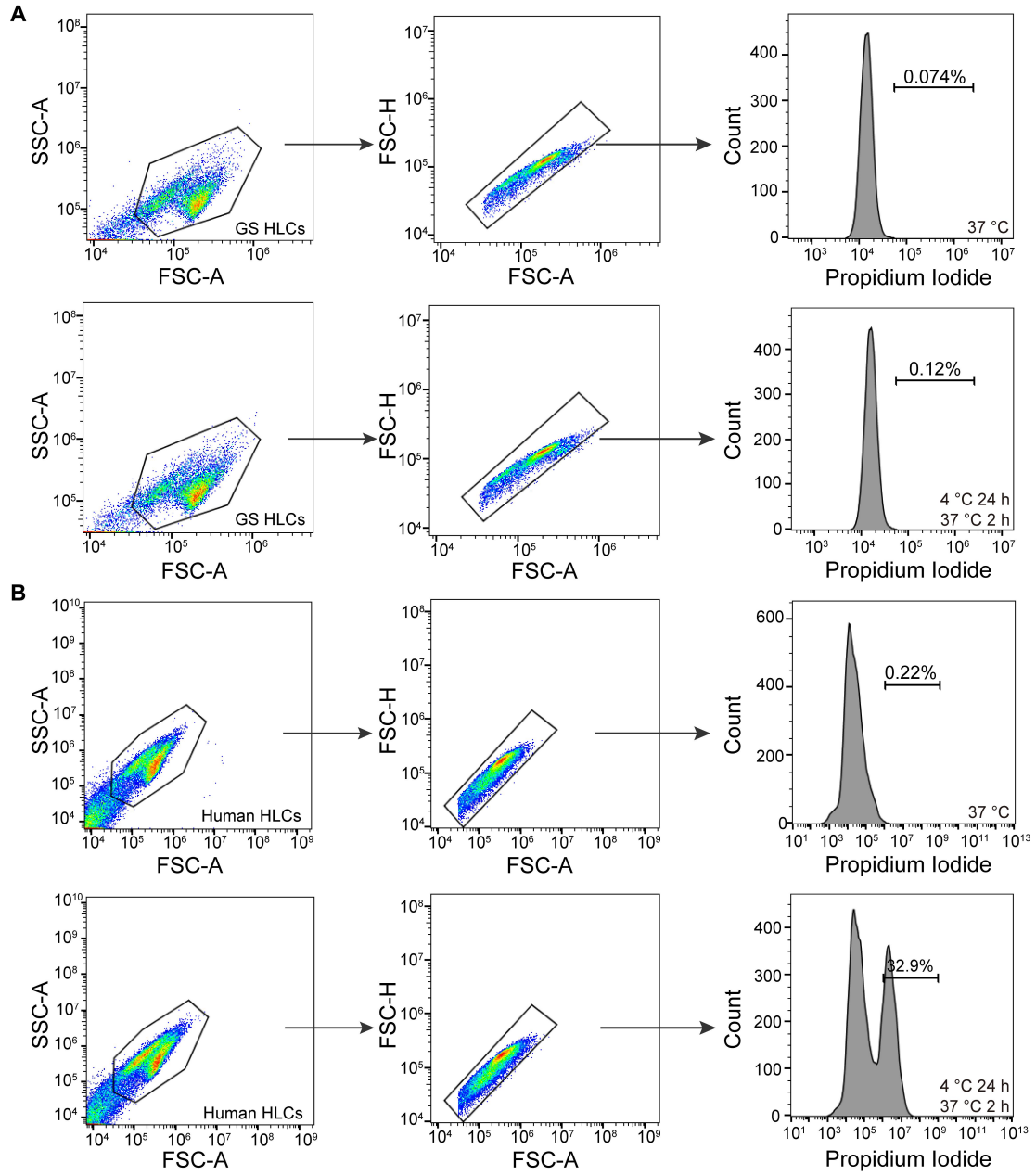


Figure S6. Gating strategy of flow cytometry in characterizing propidium iodide

(PI)-positive cells. Gating strategy of PI in GS **(A)** and human **(B)** HLCs at indicated conditions analyzed by flow cytometry. **(C)** Quantification of PI-positive cells in GS and human HLCs (n = 3). Data are expressed as mean \pm SEM; Student's t-test between two comparisons; *P* value is indicated.

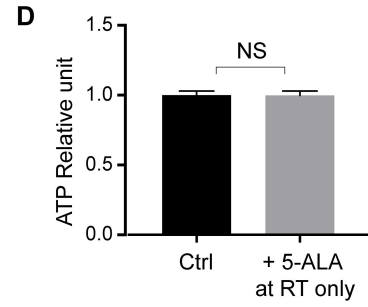
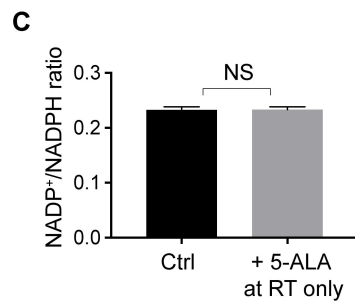
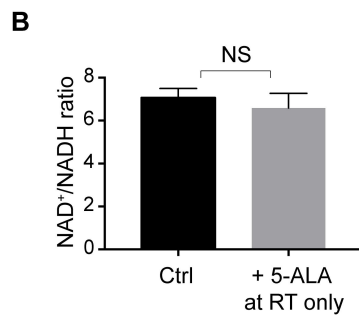
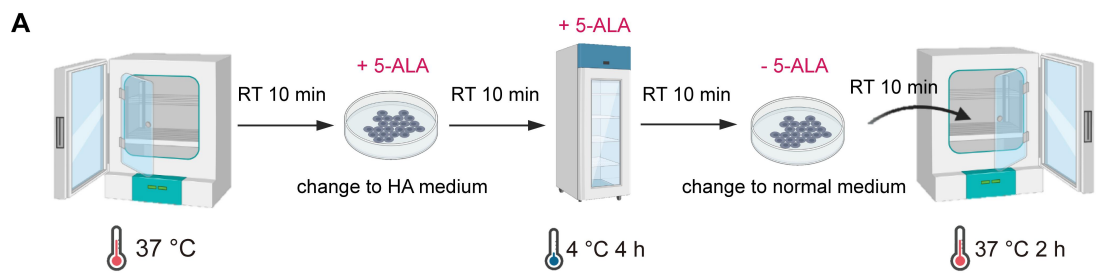


Figure S7. Effects of 5-ALA supplement to human HLCs. (A) Schematic diagram of cold incubation and rewarming of human HLCs with or without 5-ALA (see **Methods**). Incubation with 1 mM 5-ALA at room temperature (RT) for 10 min only showed little effect on NAD⁺/NADH ratio (**B**), NADP⁺/NADPH ratio (**C**) and ATP level (**D**) in human HLCs (n = 3). Data are expressed as mean ± SEM; Student's *t*-test between two comparisons; NS: not significant.

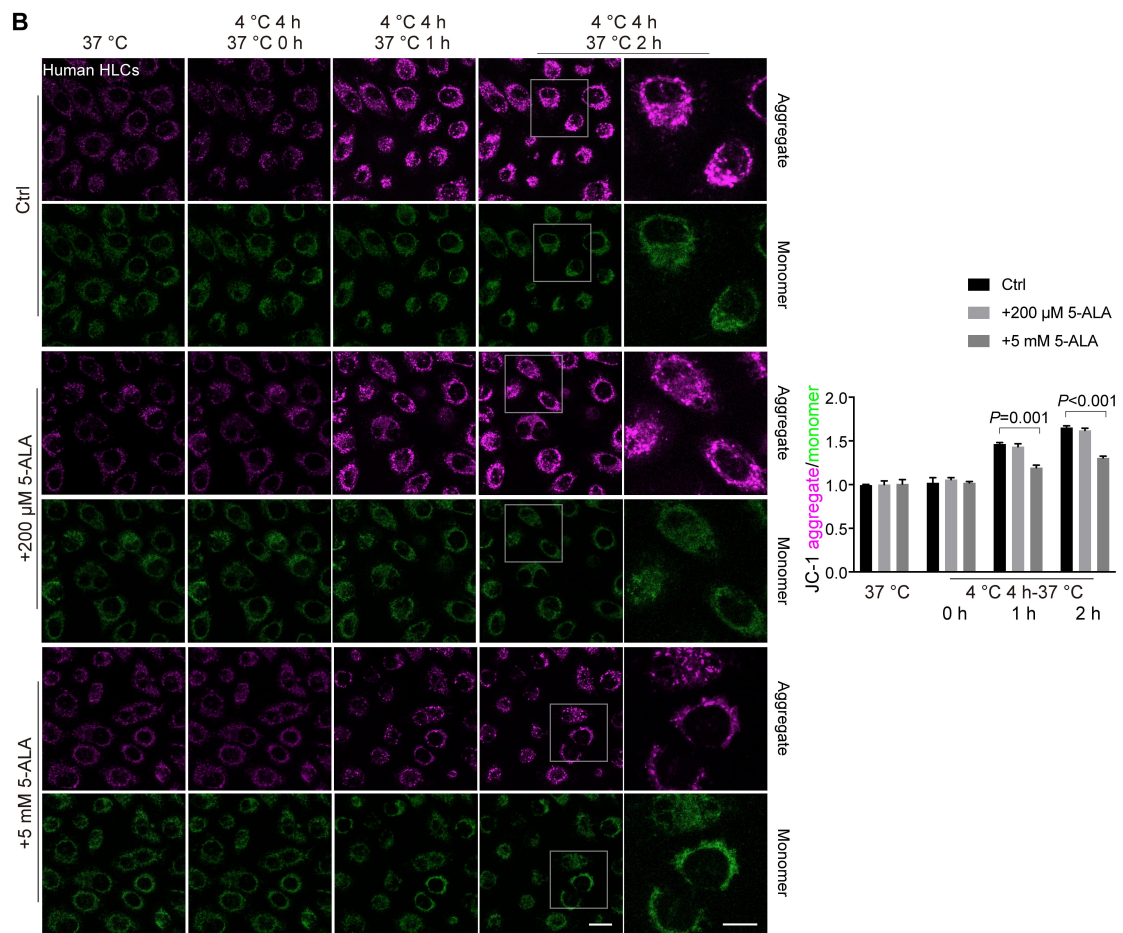
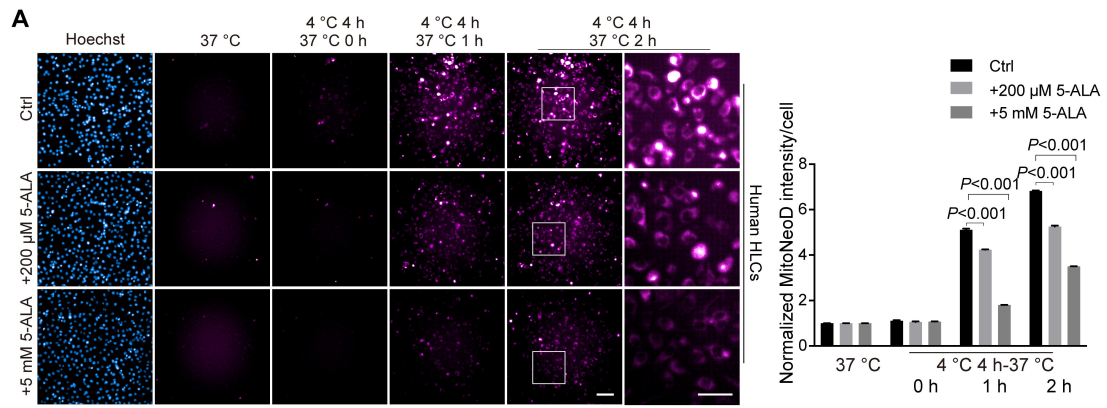


Figure S8. Dose-effects of 5-ALA treatments on mitochondrial ROS and mitochondrial membrane potential ($\Delta\psi_m$) in human HLCs during rewarming. (A) Left: automatic high-content imaging of MitoNeoD fluorescence in human HLCs during rewarming; scale bars: 100 μm ; Right: quantification of MitoNeoD intensity per cell ($n = 3$ experiments). (B) Left: live imaging of JC-1 aggregate- and monomer-fluorescence to assess $\Delta\psi_m$ in human HLCs at annotated conditions during rewarming; scale bars: 20 μm ; Right: quantification of JC-1 aggregate/monomer intensity ($n = 3$ experiments). Data are expressed as mean \pm SEM; one-way ANOVA followed by Dunnett multiple-comparisons test versus ctrl group; P values are indicated.

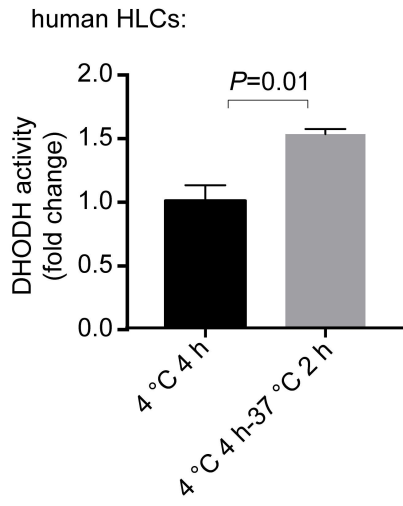
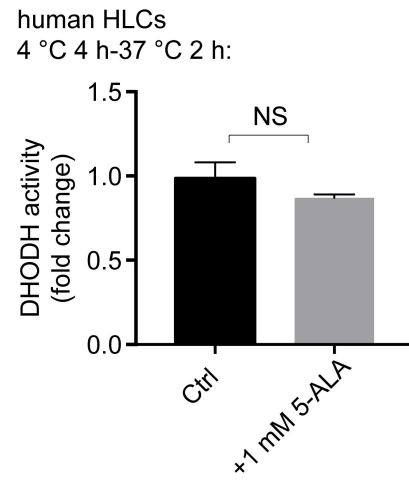
A**B**

Figure S9. DHODH activities in human HLCs. (A) Rewarming-enhanced DHODH activity in human HLCs following 4-h cold incubation (n = 3). (B) Treatment with 1mM 5-ALA had no significant effect on DHODH activity in rewarmed human HLCs (n = 3). Data are expressed as mean \pm SEM; Student's *t*-test between two comparisons; *P* value is indicated; NS: not significant.

Table S1. Characteristics of human liver donors.

Sample number	Age	Gender	Height (cm)	Weight (kg)	BMI (kg/m ²)	Cause of death	Previous condition
1	35	Male	165	70	25.7	Stroke	Not reported
2	11	Male	135	40	21.9	Head trauma	Not reported
3	25	Male	174	60	19.8	Stroke	Not reported
4	42	Female	158	58	23.2	Stroke	Hypertension
5	45	Male	173	75	25.1	Head trauma	Not reported
6	25	Male	173	60	20.0	Head trauma	Not reported
7	39	Male	165	60	22.0	Head trauma	Not reported
8	49	Male	175	78	25.5	Stroke	Hypertension
9	57	Male	170	68	23.5	Stoke	Not reported
10	32	Female	152	50	21.6	Anoxia	Not reported

BMI, body mass index.

Table S2. Other reagents.

Reagents	Catalog #	Supplier
Matrigel hESC-Qualified Matrix	354277	Corning, USA
mTeSR1 Complete Kit	85850	Stem Cell Technologies, Canada
Human Hepatocyte Medium & Bullet kit (CC-3199 & CC-4182)	CC-3198	Lonza, Switzerland
Fetal Bovine Serum	1099141C	Thermo, USA
Hibernate-A medium	A1247501	Thermo, USA
low-glucose Dulbecco's Modified Eagle Medium	C11885500BT	Thermo, USA
Accutase Cell Dissociation Reagent	A1110501	Thermo, USA
6-well cell culture plate	353046	Falcon, USA
RPMI 1640 Medium	11875093	Thermo, USA
B-27 Supplement(50X)	17504044	Thermo, USA
CHIR-99021 (CT99021)	S1263	Selleck, USA
Y27632	HY-10071	MCE, USA
Activin A	AF-120-14E-1000	PeptoTech, USA
Advanced F12	16234010	Thermo, USA
GlutaMAX Supplement	35050061	Thermo, USA
Penicillin-Streptomycin	15140-122	Thermo, USA

Human HGF	100-39	PeproTech, USA
Oncostatin M	300-10	PeproTech, USA
Dexamethasone	D4902	Sigma, USA
Paraformaldehyde	30525-89-4	Sigma, USA
Bovine serum albumin (BSA)	V900933	Sigma, USA
Triton X-100	T8787	Sigma, USA
ALEXA FLUOR 488 DONKEY	A21206	Invitrogen, USA
ALEXA FLUOR 594 DONKEY	A21203	Invitrogen, USA
ALEXA FLUOR 647 DONKEY	A31573	Invitrogen, USA
DAPI	D9542	Sigma, USA
Hoechst 33342	H3570	Thermo, USA
RNeasy Mini Kit	74104	Qiagen, Germany
cDNA Reverse Transcription Kit	11117831001	Roche, Germany
AceQ Universal SYBR qPCR Master Mix	Q511-02	Vazyme, China
Mammalian protein extraction Reagent	78501	Thermo , USA
Protease Inhibitor Cocktail	87786	Thermo , USA
Pierce BCA Protein Assay Kit	23227	Thermo , USA
Immobilon-P PVDF, 0.45 μm	IPVH00010	Millipore, Germany
Skim milk	232100	BD, USA
Immobilon Western Chemiluminescent HRP Substrate (ECL)	P90719	Millipore, Germany
PAS staining kit	3952	Sigma, USA
Indocyanine Green	1340009	Sigma, USA
BODIPY 493/503	D3922	Thermo , USA
Cell Counting Kit-8	CK04	Dojindo, Japan
Propidium iodide	P4170	Sigma, USA
JC-1	C2005	Beyotime, China
MitoNeoD	563761	Medkoo, USA
NAD/NADH-Glo Assay kit	G9071	Promega, USA
NADP/NADPH-Glo Assay kit	G9081	Promega, USA
Luciferase Assay System	E1500	Promega, USA
DHO	D7128	Sigma, USA
DCPIP	D1878	Sigma, USA
Rotenone	R8875	Sigma, USA

Antimycin A	A8674	Sigma, USA
NaN ₃	S2002	Sigma, USA
Cytochrome c	C2867	Sigma, USA
decylubiquinone	D7911	Sigma, USA
Electron transport chain Complex IV activity assay kit	BC0940	Acmecc, China
5-Aminolevulinic acid hydrochloride	HY-N0305	MCE, USA
Krebs-Henseleit bicarbonate buffer	K3753	Sigma, USA
DMEM/F12	36254	Stem Cell Technologies, Canada
Knockout Serum Replacement	A3181502	Thermo , USA
Non-Essential Amino Acids	11140-050	Thermo , USA
L-Glutamine	25030-081	Thermo , USA
L-Ascorbic acid	HY-B0166	MCE, USA
b-FGF	233-FB-025	R&D , USA
University of Wisconsin solution	SPS-1	Organ Recovery Systems, USA
In Situ Cell Death Detection Kit	11684795910	Roche, USA
p-dimethyl aminobenzaldehyde	100-10-7	Sigma, USA
glacial acetic acid	64-19-7	Sigma, USA
perchloric acid	7601-90-3	Sigma, USA
porphobilinogen	487-90-1	Sigma, USA
Amicon Ultra-15 Centrifugal Filter Unit	UFC9050	Millipore, Germany

Table S3. Sequences of qPCR primers and siRNAs.

qPCR target genes	5' primer	3' primer
<i>OCT4</i>	CAAACGACCATCTGCCGCT TT	GGTTCTCATTGTTGTCTGCT TCCTC
<i>NANOG</i>	GGAGCAATCAGACCTGGA ACAAC	CTCCAAGACTGGCTATTCC AAGACT
<i>SOX17</i>	ACCTTCACAATGCTGAGTT GAG	GGTACTTGTAGTTGGGATG GTCT
<i>GATA4</i>	TACGCATCTCCTGTCAGCC AGT	TGACTCTCAGCCAAGACCA GACT
<i>FOXA2</i>	CGCCTTCAATCATCCTTTCT CCATC	CTGTTTCGTAGGTCTTGAGG TCCATT
<i>AFP</i>	GGCATGAAGTGAATCCTGT	TGGTGGAGGAACATAGGTC

	GAACC	TCATCT
<i>HNF4A</i>	GGGTGTCCATTCGCATCCT TGA	GAGGCAGGCGTACTCATTG TCAT
<i>CK18</i>	AGAACCGAGAGGAGCTGG ACAA	AAGGACTGGACTGTGCGTC TCA
<i>CK19</i>	GGCATGAAGTGAATCCTGT GAACC	TGGTGGAGGAACATAGGTC TCATCT
<i>TBX3</i>	AGGAGACAGGAACTTCGG ATGAGT	AGTGGACACTGCTGGTGAG GAA
<i>ALB</i>	GGTGATATGGCTGACTGCT GTG	AGTGGAGGGATGGTAGGA GTATCT
<i>AAT</i>	CACCACTGCTCTTTCATTC TTCCT	GCTCAGTCCACTTGTCCAA ATTGTC
<i>APOA1</i>	CGGCATTTCTGGCAGCAAG ATG	GCAGAGGTTTCAAATTGGG TCACA
<i>TTR</i>	GCTTCTCACCATCTACTCCT CCTC	TTCACAGACACCTCCACAG CAG
#1si <i>ALAS1</i>	CAGCAACGTCTTCTGCAA	
#2si <i>ALAS1</i>	CCAATGACTCAACCCTCTT	

Table S4. Primary antibodies.

Antibody	Catalog #	Supplier	Concentration
SOX17	sc-130295	Santa Cruz	IF 1:50 WB 1:200
GATA4	sc-25310	Santa Cruz	IF 1:50 WB 1:200
HNF4a	3113	CST	IF 1:1000
AFP	sc-51506	Santa Cruz	IF 1:50 WB 1:200
AAT	sc-59438	Santa Cruz	IF 1:200
ALB	CLF301-2	CEDARLANE	IF 1:1000
ALB	sc-271605	Santa Cruz	WB 1:200 FCM 1:200
OCT4	sc-5279	Santa Cruz	WB 1:200
ACTB	4970S	CST	WB 1:1000
CYP3A4	Sc-53850	Santa Cruz	FCM 1:200
4-HNE	Ab46545	Abcam	WB 1:1000

Supplementary methods

RNA sequencing

Total RNA was prepared from isolated perfused rat livers in UW solution group or UW + 5-ALA group. A total amount of 1 µg RNA per liver was used as input material. The NEBNext Ultra™ RNA Library Prep Kit for Illumina (NEB, USA) was used to generate cDNA libraries according to manufacturer's protocol and index codes were added to attribute sequences to each sample. The products were purified (AMPure XP system) and library quality was assessed on Bioanalyzer 2100 system (Agilent USA). Clustering of the index-coded samples was performed using TruSeq PE Cluster Kit v3-cBot-HS (Illumina, USA) on cBot Cluster Generation System. After cluster generation, the prepared libraries were sequenced on an Illumina Novaseq platform and 150 bp paired-end reads were generated.

Quality control

Raw data (raw reads) of fastq format were firstly processed through in-house perl scripts. In this step, clean data (clean reads) were obtained by removing adapter, and excluded reads containing ploy-N and low-quality from raw data. At the same time, Q20, Q30 and GC content the clean data were calculated. All the downstream analyses were based on the clean data with high quality.

Reads mapping to the reference genome

Reference genome and gene model annotation files were downloaded from ensemble website directly[1]. Index of the reference genome was built using Hisat2 v2.0.5 and paired-end clean reads were aligned to the reference genome using Hisat2 v2.0.5[2].

Quantification of gene expression level

For quantification of gene expression, reads pairs were excluded that have their two ends mapping to different chromosomes or mapping to same chromosome but on different strands, and only count read pairs that have both ends aligned. Only the reads

aligned to exons, and with the mapping quality score larger than 10 were counted using the featureCounts v2.0.1 package[3].

Differential expression analysis

Differential expression analysis was performed by DESeq2 R package (1.26.0)[4] using a model based on the negative binomial distribution. The resulting P-values were adjusted using the Benjamini and Hochberg's approach for controlling the false discovery rate.

Heatmap and Enrichment analysis

Genes with the adjusted P-value < 0.05 and $\log_2\text{Foldchange} > 0.5$ were considered to be significantly differentially expressed. Heatmap of genes were plotted using R, and functional enrichment analyses of differentially expressed genes were performed by the clusterProfiler R package(3.14.3)[5].

References

1. Zerbino DR, Achuthan P, Akanni W, Amode MR, Barrell D, Bhai J, et al. Ensembl 2018. *Nucleic Acids Res.* 2018; 46: D754-D61.
2. Kim D, Paggi JM, Park C, Bennett C, Salzberg SL. Graph-based genome alignment and genotyping with HISAT2 and HISAT-genotype. *Nat Biotechnol.* 2019; 37: 907-15.
3. Liao Y, Smyth GK, Shi W. featureCounts: an efficient general purpose program for assigning sequence reads to genomic features. *Bioinformatics.* 2014; 30: 923-30.
4. Love MI, Huber W, Anders S. Moderated estimation of fold change and dispersion for RNA-seq data with DESeq2. *Genome Biol.* 2014; 15: 550.
5. Yu G, Wang LG, Han Y, He QY. clusterProfiler: an R package for comparing biological themes among gene clusters. *OMICS.* 2012; 16: 284-7.